Solar Physics (2026) 301:68
https://doi.org/10.1007/s11207-026-02654-w

RESEARCH

The Sun as a Rosetta Stone for Understanding Star–Planet Interactions

Maria Pia Di Mauro[1] · **Camilla Pezzotti**[1,2] · **Raffaele Reda**[3] · **Nuno Moedas**[1] · **Luca Giovannelli**[3]

Received: 5 June 2025 / Accepted: 4 April 2026
© The Author(s) 2026

Abstract

The Sun serves as a unique and invaluable reference point, or "Rosetta Stone", for the study of other planetary systems. As the only star that can be observed with high spatial and temporal resolution, the Sun provides critical insight into stellar structure and activity, exoplanet formation, and star–planet interactions.

We demonstrate the efficiency of a multi-disciplinary approach to interpret phenomena observed in distant exoplanetary systems by analogy with the Sun-Earth system. By applying the Star-Planet Interaction (SPI) code to a highly accurate model of the host star constrained by asteroseismic observations and empirical stellar wind proxies, we show that it is possible to quantify the impact of the star's rotation and gravitational-tidal interaction on the long-term evolution of exoplanets including the resulting atmospheric loss and its implications for habitability.

Here we show results obtained for the case of the Sun and provide a powerful framework for interpreting the habitability potential of exoplanetary systems across the Galaxy.

Keywords Helioseismology · Magnetic activity · Space-weather · Space climate · Solar-like stars

✉ M.P. Di Mauro
maria.dimauro@inaf.it

C. Pezzotti
camilla.pezzotti@uliege.be

R. Reda
raffaele.reda@roma2.infn.it

N. Moedas
nuno.martinsmoedas@inaf.it

L. Giovannelli
luca.giovannelli@roma2.infn.it

1 INAF-IAPS, Via del Fosso del Cavaliere 100, 00133 Rome, Italy

2 STAR Institute, Universitè de Liège, Liège, Belgium

3 Dipartimento di Fisica, Università degli Studi di Roma Tor Vergata, Via della Ricerca Scientifica 1, 00133 Rome, Italy

Published online: 08 May 2026

1. Introduction

Due to its proximity and the wealth of observational data available, the Sun represents the best laboratory for studying the complex interplay between stars and their orbiting planets. In particular, the study of the Sun–Earth system can provide a detailed framework for modelling the circumplanetary environments that other exoplanets may experience and in particular to evaluate the conditions that might allow habitability.

In order to investigate the Sun-Earth interaction, it is necessary to consider different physical processes. These include the presence of a strong planetary magnetic field which shields against the solar magnetic activity, solar wind and energetic particle fluxes (See et al. 2014; Varela et al. 2023). Moreover, variations in solar irradiance are known to have measurable impacts on both magnetospheric and atmospheric dynamics (see e.g. Airapetian et al. 2020; Eyelade et al. 2024).

In addition to radiative and magnetic influences, gravitational-tidal interactions between the Sun and Earth play a critical role in maintaining Earth's long-term stability and habitability. These forces regulate the planet's orbital eccentricity, obliquity, and rotational period. Tidal interactions can also generate internal heating, which supports geological activity and sustains a magnetic field to protect the atmosphere, enabling surface habitability.

This manuscript examines the Sun's role as a reference standard for exoplanetary science, emphasizing its value in modelling solar-like stars, stellar magnetic activity, planetary climate regulation and the physical mechanisms that govern star–planet interactions.

While the individual components of our strategy regarding seismic characterization and empirical stellar-wind proxies have been introduced in Reda et al. (2022) and Reda et al. (2023), here we integrate these elements into a unified framework and we show the simulation relative to the Sun. The novelty result is obtained by combining precise asteroseismic ages and solar-calibrated wind histories with the model of the long-term radiative and gravitational interaction, in order to provide a complete timeline from disk dissipation to the current age and predict atmospheric erosion of orbiting planets.

We point out that adopting the Sun as a "Rosetta stone" necessarily limits the applicability of the present strategy to stars which similarly to the Sun are characterized by an outer convective envelope capable of exciting solar-like oscillations, and whose magnetic activity can be attributed to a dynamo mechanism generated by the interaction between differential rotation and convective motions (Parker 1955; Charbonneau 2020). In practice, this restricts the applicability of our study to stars, mainly G spectral type, with masses in the range $(0.8-1.2)\ M_{\odot}$, stellar radii $\approx 1 R_{\odot}$, and photospheric temperatures of about $5000-6000$ K.

This manuscript is structured as follows: in Section 2 we describe the stellar characterization strategy with particular emphasis on the role of helio- and asteroseismic constraints in determining stellar mass, radius, age, and internal rotation properties relevant for star–planet interaction studies; Section 3 focuses on the characterization of stellar magnetic activity and wind properties, introducing the solar–calibrated empirical proxies employed to reconstruct the long-term evolution of the stellar wind and its interaction with planetary magnetospheres; in Section 4 we present the Star–Planet Interaction (SPI) framework and describe how radiative, magnetic, and gravitational effects are coupled to model the co-evolution of the host star and its planets. Finally, in Section 5 we present the results and in Section 6 we discuss the physical implications of the framework, its limitations, and its relevance for assessing the long-term habitability of terrestrial planets orbiting solar-like stars.

2. Solar-Calibrated Characterization of Host Stars and Target Selection

In order to ensure that the physical mechanisms governing star–planet interactions can be interpreted in close analogy with the Sun–Earth system, we aim to identify and characterize a physically consistent sample of suitable targets. Rather than selecting solar analogues solely on the basis of fundamental parameters, our approach focuses on stars that share a similar evolutionary phase, rotation rate, and magnetic activity regime. This selection strategy ensures that both stellar structure and magnetically driven processes can be meaningfully compared with the solar case.

The characterization of exoplanets and their environments therefore starts from a precise and accurate determination of the fundamental properties of the host star. Stellar parameters such as mass, radius, age, and rotation directly affect planetary evolution, atmospheric escape, and habitability conditions. Among these, stellar age and evolutionary phase are fundamental parameters for reconstructing the formation history and long-term evolution of planetary systems (Pont 2009; Soderblom 2010).

In this context, helioseismology offers a fundamental reference for characterizing the internal structure, dynamics, and evolution of the Sun, whereas asteroseismology extends this diagnostics to other solar-like stars, allowing a physically consistent comparison of their properties.

2.1. From Helio- to Asteroseismology as Tools for Host-Star Characterization

Helioseismology has provided an unprecedented level of detail on the solar internal structure and dynamics, enabling major advances in the modelling of stellar physics, including the equation of state, opacities, nuclear reaction rates, and the treatment of convection. In particular, helioseismic inversions (Schou et al. 1998) have shown that the surface latitudinal differential rotation extends throughout the convective envelope, while the radiative interior rotates almost rigidly. The transition between these two regimes occurs in the tachocline, a thin shear layer located at r=(0.713±0.001) $R_\odot$ (Basu and Antia 1997), which is widely believed to play a key role in the generation of the solar magnetic dynamo.

The Sun therefore provides a natural benchmark for stellar modeling. To illustrate the evolution of internal structure and convective properties, the top panel of Figure 1 shows the evolutionary track calculated for the 1 $M_\odot$ Solar Standard Model, which best fits all the available observational constraints including helioseismic individual frequencies. In our models, two basic assumptions are that the star was initially chemically homogeneous and that during its evolution up to the present solar age mass loss has been negligible.

The level of physical understanding achieved for the Sun provides the reference framework against which stellar models of solar-like stars can be calibrated and validated. Building on this foundation, asteroseismology now enables similar investigations for thousands of stars with properties comparable to those of the Sun, extending studies of star–planet interactions well beyond the solar system.

The characterization of solar-like stars relies on the detection of solar-like oscillations and detailed analysis of *Kepler* or Transiting Exoplanet Survey Satellite (TESS) photometric time series. For individual stars, the precision with which stellar parameters can be estimated depends on the quality of the available asteroseismic information (Lundkvist et al. 2018). Scaling relations based on global asteroseismic parameters of the oscillation spectrum typically yield radii with 3 – 5% precision, masses within 7 – 10%, and ages with uncertainties of 20 – 30% or more. In order to achieve higher precision, of the order of $\simeq$ 1 – 2% in ra-

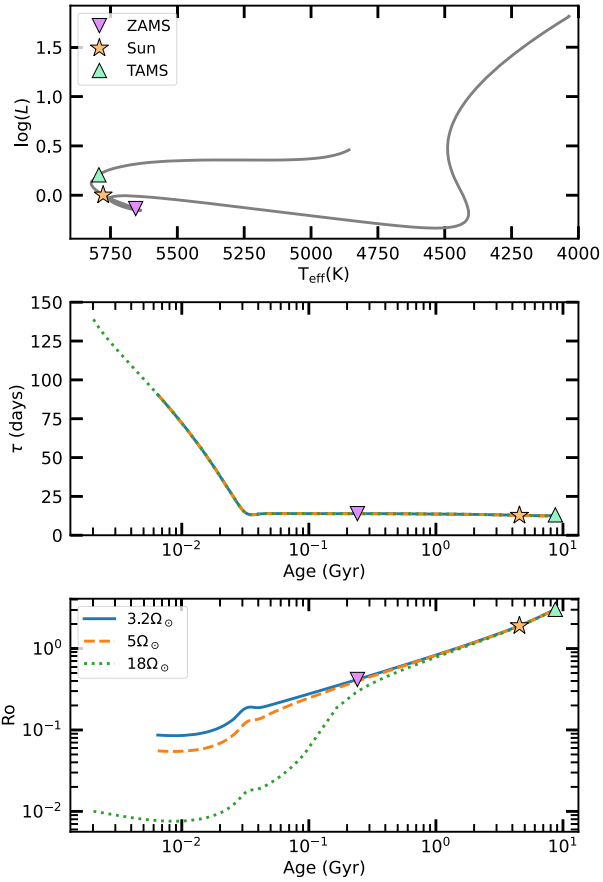

Figure 1 Top panel: HR diagram of the evolutionary track of a Solar Standard Model computed with the Code Liégeois d'Évolution Stellaire (CLES) code from the pre-main sequence to the end of subgiant stage. Middle panel: Temporal evolution of the local convective turn over time in the stellar models. Bottom panel: Temporal evolution of the Rossby number in the stellar models for a slow, moderate, and fast rotator Sun, calculated with the above τ. In both panels we marked different points of evolution, zero-age main sequence (ZAMS) (pink down triangle), present Sun (yellow star), and the terminal-age main sequence (TAMS) (acqua marine up triangle).

dius, $\simeq 5\%$ in mass, and $\simeq 10\%$ in age, it is required detailed evolutionary modelling of the stellar structure, constrained by individual oscillation frequencies together with non-seismic atmospheric parameters, as proved by Lebreton and Goupil (2014) and Miglio et al. (2017) by comparing the results against independent measurements, such as radii and masses from binary systems.

Beyond fundamental stellar parameters, asteroseismology provides unique diagnostics of the internal rotation profile. Observations from the *Kepler* mission have revealed that the internal rotation of solar-like stars evolves significantly during stellar evolution. In particular, the mean core rotation decreases substantially as stars ascend the red-giant branch, providing direct evidence of angular momentum redistribution within stellar interiors (Mosser et al. 2012; Deheuvels et al. 2014). Moreover, seismic analyses have revealed the presence of sharp rotational shear layers in evolved stars. For example, Di Mauro et al. (2018) identified an angular velocity gradient located between the helium core and the hydrogen-burning shell in red giants, analogous to the tachocline observed in the Sun. These results demonstrate that shear layers separating regions of different rotational regimes are a common feature of solar-like stars and suggest that dynamo mechanisms similar to the solar one may operate across different evolutionary phases.

Asteroseismology can directly probe the internal structure and rotation of stars but, as we will see in the next section, magnetic activity is controlled by the interplay between

rotation and convection and the efficiency of dynamo action depends critically on the relative timescales of rotational and convective processes.

2.2. The Rossby Number as a Proxy for Solar-like Magnetic Activity

The solar magnetic activity is closely linked to the internal dynamo, which as first suggested by Larmor (1919), is originated by a $\alpha - \Omega$ mechanism, where the α-effect arises from helical turbulence (Parker 1955), while the Ω-effect results from the Sun's differential rotation, both in latitude, with equator rotating faster than the poles, and in radial direction (Schou et al. 1998).

The dynamo is thought to operate in the tachocline, the thin shear layer at the interface between the radiative interior and the convective envelope. Its precise location can be determined only in the Sun (e.g. Di Mauro, Dziembowski, and Paternó 1998) and, exceptionally, in the red-giant star KIC 4448777 (Di Mauro et al. 2018). In other solar-like stars, the tachocline itself cannot be resolved, but the depth of the convective envelope can be inferred with comparable precision through detailed seismic modeling, provided a sufficiently large set of oscillation modes is available. This makes the base of the convection zone a natural reference point for defining quantities relevant to stellar dynamos across stars similar to the Sun.

In order to define and compare the magnetic activity status between the Sun and the other stars in a physically meaningful way, it is common to use the so-called Rossby number Ro, a dimensionless parameter that quantifies the relative importance of rotation and convection. This quantity gives insight into the expected activity levels and magnetic field generation via the dynamo process. According to Noyes et al. (1984), it is defined as:

$$\mathrm{Ro} = \frac{P}{\tau} \tag{1}$$

where $\mathrm{P} = 2\pi / \Omega$ is the surface stellar rotational period, Ω is the angular velocity, and τ is the convective turnover time, defined as the characteristic timescale of convective cells motion within the stellar convective zone.

Stars with $\mathrm{Ro} \ll 1$, such as fast rotators or stars with deep convective zones (e.g. M dwarfs) are dominated by Coriolis forces, which organize convective flows and enhance shear, resulting in an efficient dynamo. On the contrary, a large Rossby number ($\mathrm{Ro} \gg 1$) indicates that Coriolis forces have minimal time to act on a convective element, leading to weaker dynamo action, as in slow rotators or stars with thinner convective zones (F-type stars). In general, as a star evolves from the zero-age main sequence (ZAMS), the Rossby number is expected to increase with the rotational period due to magnetic braking, where the stellar wind carries away angular momentum (Skumanich 1972) (see lower panel of Figure 1).

Stellar dynamos are observed to operate in two major regimes: the saturated and non-saturated one. For Rossby numbers below a critical threshold, $\mathrm{Ro_{cri}}$, typically of the order of 0.1 for τ evaluated locally at the base of the convective zone, stars populate the saturated regime. In the saturated regime, the correlation between magnetic activity indicators and Rossby number becomes flat (e.g. Pizzolato et al. 2003; Wright et al. 2011; Johnstone, Bartel, and Güdel 2021), showing no dependence on stellar rotation. This behaviour has been interpreted as evidence that the dynamo operates at maximum efficiency, possibly due to saturation of the surface filling factor of active regions, or as a consequence of enhanced angular-momentum loss through magnetized stellar winds (Wright et al. 2011).

For $\mathrm{Ro} > \mathrm{Ro}_{\mathrm{cri}} \approx 0.1$, stars enter the non-saturated regime, which is typical of more slowly rotating solar-type stars. In this regime, magnetic activity decreases with increasing Rossby number, reflecting the progressively reduced efficiency of rotationally driven convection on the dynamo (Noyes et al. 1984). Recent observations from *Kepler* (Santos et al. 2024) have refined this picture, showing that the transition between saturated and non-saturated regimes depends not only on rotation but also on stellar mass and evolutionary stage: as solar-type stars evolve, they lose angular momentum through magnetic braking and gradually move into the non-saturated regime. This result provided key tests for dynamo theory and for models of stellar spin-down.

In the Sun the surface rotational period can be measured directly following the sunspots movement or by employing helioseismic inversion. In other stars the rotational period is typically measured by employing spectroscopic observations, asteroseismic time series or photometric light curve modulation.

The convective turnover time cannot be measured directly, so it can be estimated from stellar theoretical models or by using empirical relations based on different stellar properties (see e.g. Noyes et al. 1984; Rasio et al. 1996; Villaver and Livio 2009; Wright et al. 2011; Cranmer and Saar 2011; Wright 2018).

The convective turnover time, derived from 1D stellar models, depends sensitively on the adopted input physics, in particular the treatment of convection, usually described by the mixing-length formalism (Böhm-Vitense 1958), as well as the surface metallicity, opacity, and even the specific definition of τ. In fact, τ can be defined according to different prescriptions, which lead to systematic differences by factors two or more in the derived Rossby numbers. Here we give the main definitions, though care is needed when making comparisons: the local turnover time is $\tau_{\mathrm{bcz}} = H_p/v_{\mathrm{bcz}}$ where H_p and v_{bcz} are respectively the pressure scale height and the convective velocity of a cell evaluated at the base of the convection zone (bcz) (e.g. Böhm-Vitense 1958); the global or integrated turnover time, $\tau_{\mathrm{g}} = \int_{r_{\mathrm{bcz}}}^{R} \frac{dr}{v(r)}$ represents the time required for a convective cell to cross the convection zone (e.g. Mathur et al. 2014); the average turnover time is $\tau_{cz} = d_{cz}/\overline{v_{cz}}$ where d_{cz} is the thickness of the convective envelope and $\overline{v_{cz}}$ the average velocity of a convective cell within the convective region (Brun and Browning 2017). More modern approaches relying on 3D radiative-hydrodynamic (RHD) simulations have been able to provide more accurate convective velocities and pressure scale heights (Nordlund, Stein, and Asplund 2009; Magic, Weiss, and Asplund 2015). However, these simulations cannot be applied to evolving stellar models, as they would require prohibitively long computing times.

The semi-empirical relations of the convective turnover time were first introduced by Noyes et al. (1984), who derived a calibration between τ and the $(B - V)$ color index using Ca II H and K activity measurements and surface rotational periods of nearby solar-type stars. This calibration has been extensively adopted in studies of stellar dynamos and activity-rotation relations, because of its simplicity and its applicability to large photometric samples. More recently, Jao et al. (2022) have extended these calibrations using modern datasets, refining the dependence of τ on color indices for cool dwarfs. Despite their practical value, these relations remain subject to large uncertainties: stars with similar colors and masses can display variations in activity levels that translate into a dispersion of more than 30% in the inferred τ. To give a comparison, the calibration of Noyes et al. (1984) for the Sun yields $\tau_{N_\odot} \approx 12$ days, and $\mathrm{Ro}_{N_\odot} \approx 2$, while stellar structure models give a local turnover time of $\tau_{c_\odot} \approx 15.6$ days ($\tau_{g_\odot} \approx 38.2$ days) and $\mathrm{Ro}_\odot \approx 1.6$ (Landin, Mendes, and Vaz 2010).

More recently, it has been proved that a good method to improve the Rossby number estimates is to use both the two approaches, trying to tie relations calibrated on a sample

of stars with known rotation rates and magnetic activity indicators to computed stellar evolutionary models. For example, Corsaro et al. (2021), using asteroseismic analysis of well-characterized *Kepler*'s Legacy solar-like stars, derived a new calibration of the convective turnover timescale and Rossby number, also confirmed by Metcalfe et al. (2024).

In this manuscript the value of τ has been estimated locally, at the base of the convective zone, by using stellar models computed with the CLES (Code Liégeois d'Évolution Stellaire) stellar evolution code, with the detailed physics described in Scuflaire et al. (2008) and adopting the formula given by Rasio et al. (1996) and Villaver and Livio (2009). The middle and lower panels of Figure 1 show the corresponding values of the local τ and Ro as they vary during the evolution for three standard solar models, constrained on helioseismic observations, evolving from the pre-main sequence through the ZAMS, calculated by assuming three different initial rotation rates: low $\Omega_{\rm in} = 3.2\ \Omega_\odot$, moderate $\Omega_{\rm in} = 5\ \Omega_\odot$ and fast $\Omega_{\rm in} = 18\ \Omega_\odot$, respectively, with the surface rotation rate of the Sun at solar age $\Omega_\odot = 2.9 \times 10^{-6}$ rad/s. According to our modelling, the Rossby number of the present-day Sun is $\mathrm{Ro}_\odot = 25/13.92 = 1.79$, which is consistent with the ones obtained previously (Noyes et al. 1984; Landin, Mendes, and Vaz 2010).

Figure 1 shows that, for the Standard Solar Model, τ remains nearly constant along all the main sequence evolution, while the Rossby number increases with age independently of the initial rotation rate. This indicates that at least theoretically the Sun in the main sequence (MS) does not retain memory of its original and pre-main sequence (PMS) rotational conditions.

Hence, a practical criterion to select stars with magnetic activity properties similar to the Sun is to consider stars with Rossby number $\mathrm{Ro} \geq 1$, as pointed out by Reinhold et al. (2019). By studying the appearance of activity signatures in contemporaneous photometric and chromospheric time series of 30 Sun-like stars, they found that the transition from spot- to faculae-dominated activity regime occurs at a Rossby number $\mathrm{Ro} \approx 1$, which corresponds to a stellar age of $\approx$2.6 Gyr. Thus stars with $\mathrm{Ro} \leq 1$ should be spot-dominated, while stars characterized by $\mathrm{Ro} \geq 1$ should be faculae-dominated, as the Sun.

It is clear that while the Rossby number is widely used as a proxy for magnetic activity in solar-like stars, it should be noted that it does not capture the full complexity of stellar magnetic fields, nor possible variations in magnetic braking laws associated with different magnetic topologies (e.g. Garraffo et al. 2018) and wind–magnetic field coupling (Vidotto et al. 2014). Consequently, the activity–Rossby number relations adopted here should be regarded as first-order estimates for stars similar to the Sun, and only as a method to select a sample suitable for the present procedure.

3. Solar Wind-Magnetosphere Interaction

Having established a solar-calibrated framework to characterize the magnetic activity regime of solar-like stars through the Rossby number, we now move to the next key ingredient of star–planet interactions: the stellar wind.

When studying the Sun-Earth interaction, the evaluation of the solar wind effects on the near-Earth environment is one of the main processes that needs to be considered. In magnetized planets, like the Earth, the interaction between the stellar wind and the planetary magnetic field determines the structure and extent of the magnetosphere and regulates the transfer of mass, momentum, and energy into the planetary environment.

The supersonic solar wind plasma is deflected by the geomagnetic field, giving rise to a bow shock forms upstream, where the solar wind abruptly slows down, followed by the

magnetosheath, and then the magnetopause, which marks the outer boundary of the magnetosphere (Parker 1958; Dungey 1961).

The interaction between the solar wind and the magnetosphere is highly variable and is strongly influenced by solar activity in the form of coronal mass ejections (CMEs), particle fluxes, and solar flares. The solar wind can compress the magnetosphere, enhancing energy input and triggering geomagnetic storms, and, under certain conditions, can even erode or displace it. Understanding these interactions is therefore essential for any investigation aimed at studying the conditions for planetary and exoplanetary habitability.

Starting from MHD equations, it is possible to study the dynamic equilibrium between the Earth's magnetic field pressure and solar wind one. By solving this equilibrium condition, it is possible to compute the so-called magnetopause stand-off distance R_{MP}, (see e.g. Grießmeier et al. 2004; Reda et al. 2023). This quantity represents the distance from Earth at which the solar wind dynamic pressure balances the magnetic pressure of the magnetospheric cavity. In formula, R_{MP} can be expressed as:

$$R_{MP} = \left[\frac{\mu_0 f_0^2 M_E^2}{8\pi^2 \cdot 10^{-9}\, P_{dyn}} \right]^{1/6} \tag{2}$$

where P_{dyn} is the solar wind dynamic pressure in units of nPa, μ_0 is the vacuum permeability, M_E is the Earth's magnetic moment, while f_0 is a form factor to take into account for the non-spherical shape of the Earth's magnetosphere. The form factor can be usually assumed to be $f_0 = 1.16$, while $M_E = 8 \cdot 10^{22}$ Am^2, as in See et al. (2014).

Since it is not possible to measure stellar wind properties in exoplanetary systems, such equilibrium conditions need to be studied differently, combining theoretical models, numerical simulations and also taking advantage of what has been learned for the Sun-Earth interaction. The approach we propose here follows that of Reda et al. (2023), who analysed data from five solar cycles, identifying a relationship between P_{dyn} and the Ca II K index. The Ca II K index is a solar proxy that represents the chromospheric activity of the Sun, focusing specifically on the intensity of the Ca II K line at a wavelength of 393.4 nm. This linear relationship is expressed as:

$$P_{dyn}(\text{nPa}) = (\gamma_P\ \text{Ca II K} + \delta) \tag{3}$$

with $\gamma_P = 49.1 \pm 2.8$ and $\delta = -3.17 \pm 0.24$. This enables to directly estimate the wind dynamic pressure from the solar emission in the Ca II K line. Once the dynamic pressure is determined, computing the extent of the magnetosphere through Eq. 2 becomes straightforward. Figure 2 shows the extent of Earth's magnetosphere from 1970 to 2023, as derived from the Ca II K emission index (also shown). Note that when the Ca II K index increases (and consequently P_{dyn} as well), the extent of Earth's magnetosphere decreases, with an observed average time lag of approximately three years (see Reda et al. 2023, 2024), reflecting the delayed cumulative effects of solar wind modulation over the solar cycle. During periods of high solar activity, when the Ca II K index reaches values above ≈ 0.09, the magnetopause is compressed up to $R_{MP} \approx 10.5\, R_E$, corresponding to a reduction of 5 – 6% relative to the mean $R_E = 6371$ km. During low activity periods, with Ca II K index below ≈ 0.085, the magnetopause expands to $R_{MP} \approx 12\, R_E$, an increase up to 9 – 10% over the mean. Extrapolating these results to other solar-like stars, the same Ca II K–based approach can provide first-order estimates of exoplanetary magnetosphere sizes. For stars more active than the Sun, with higher Ca II indices, we can expect stronger stellar winds and correspondingly smaller magnetopause distances, potentially compressing a magnetosphere by

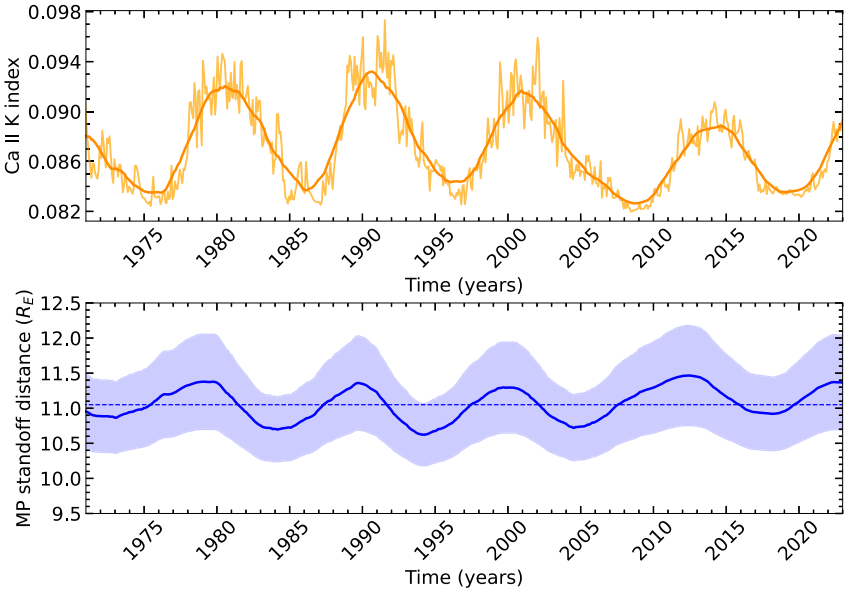

Figure 2 Top panel: Monthly averages of the Ca II K index with a superimposed 37-month smoothing. Bottom panel: The stand-off distance of Earth's magnetopause, R_{MP} (solid blue line), along with its confidence interval (shaded blue area), derived by combining Eq. 2 and Eq. 3. The dashed blue line indicates the average value for the period 1970–2023. Figure partially readapted from Reda et al. (2023).

20 – 30% relative to an Earth analogue. Conversely, for older or slower-rotating solar-type stars with lower chromospheric activity, exoplanetary magnetospheres may expand beyond the Earth's value, possibly increasing protection against stellar wind erosion. However, the exact scaling will depend on stellar mass, rotation rate, and magnetic topology, highlighting the importance of combining Ca II–derived estimates with rotational and asteroseismic constraints to refine stellar wind and magnetosphere predictions.

The advantage of this approach lies in the fact that the emission in the Ca II K lines has been monitored for thousands of stars since the 1960s, thanks to the pioneering observational campaign conducted at Mount Wilson Observatory (Wilson 1968, 1978), which was later continued at the Lowell Observatory (Hall and Lockwood 1995, 2004). However, stellar spectral observations covering these lines continue to be carried out using several spectrographs, including those of the Telescopio Internacional de Guanajuato Robótico Espectroscópico (TIGRE) at the Hamburg Observatory (Schmitt et al. 2014), the High Accuracy Radial velocity Planet Searcher (HARPS)/ESO facility (Perdelwitz et al. 2024), and the California Planet Search (CPS) at the Keck Observatory (Baum et al. 2022). The availability of these data sets for a large number of stars, combined with Sun-calibrated relationships, enables the study of the potential effects of stellar wind pressure on planets orbiting solar-like stars. The validity of this method has been demonstrated by Reda et al. (2023), where the authors, using a sample of ten stars, obtained magnetosphere sizes for Earth-analogues that are consistent with those derived by See et al. (2014) using two stellar wind models.

The Ca II K–based methodology offers the advantage of being directly applicable to a wide range of stars with long-term chromospheric monitoring. However, since it only quantifies the average stellar wind conditions, it cannot capture the detailed spatial structure and temporal variability of stellar winds. Three-dimensional MHD simulations constrained by

Zeeman–Doppler Imaging (ZDI) magnetograms (e.g. Vidotto et al. 2014; Alvarado-Gómez et al. 2016a,b; Garraffo, Drake, and Cohen 2016; Garraffo et al. 2022; Chebly et al. 2023; Vidotto et al. 2023) can provide more accurate results in this regard, including variations in stellar magnetic topology and inclination. The advantage is that while ZDI maps are only available for a few stars, the Ca II K index has been measured for a larger number of stars, so that our approach can be applied to several solar-like stars. Moreover, the empirical Ca II K approach used here, calibrated on the Sun and based solely on observational data, can be complemented by spatial wind properties derived from the more computationally demanding models listed above. In the near future, we plan to provide a more detailed comparison to assess the level of agreement between the different approaches.

Finally, we note that our framework is based on the Ca II K index to estimate the average steady-state solar wind dynamic pressure. This proxy does not explicitly account for transient events such as CMEs, which can dominate atmospheric erosion during active phases. While predicting the occurrence and properties of CMEs is beyond current observational capabilities, to partially account for such high-energy events, our Star-Planet Interaction code (see following section) adopts the maximum observed X-ray and extreme-ultraviolet (XUV) fluxes as a conservative estimate of the stellar high-energy environment.

4. Tidal and Radiative Star-Planet Interactions in Exoplanetary Systems

After having characterized the fundamental properties and magnetic activity of the host star, it is possible to proceed with the study of the long-term evolution of the star-planet system, under the simultaneous impact of gravitational-tidal and radiative interactions (e.g. Privitera et al. 2016; Rao et al. 2018; Pezzotti et al. 2025). These processes, which strongly depend on the structural and rotational properties of the host star, significantly affect different aspects of planetary evolution: gravitational-tidal interactions primarily shape orbital and rotational dynamics of the host star and planets, while radiative interactions control energy balance and mass loss from the planetary atmosphere, thus crucially determining their climate conditions.

The present simulation is based on the use of the Star-Planet Interaction (SPI) code (Privitera et al. 2016; Rao et al. 2018; Pezzotti et al. 2021, 2025), in which the evolution of a star-planet system is computed under the mutual impact of the tidal and radiative interactions, starting from the dissipation of the protoplanetary disk (≈ 10 Myr), to the current (or future) evolutionary stages of the host star.

The strategy used for the modelling consists of three major steps: firstly, we determine the optimal model of the host star by means of classical and asteroseismic constraints (see Section 1); secondly, we compute the evolutionary track of the host star by means of the Liège Stellar Evolution Code (CLES, Scuflaire et al. 2008); thirdly, we provide the evolutionary track as input to the SPI code, where the evolution of the host star surface rotation rate is computed as due to the changes in the stellar interior structure, surface magnetic braking, and tidal interactions, together with the evolution of the planetary orbit and the mass loss from its atmosphere caused by the host star high energy irradiation.

In general, while our SPI code includes gravitational-tidal interactions, we note that for Earth-analogs at 1 AU, these effects are negligible compared to radiative drivers. However, for the close-in planets targeted by missions like the PLAnetary Transits and Oscillations of stars (PLATO), or in the case of planetary systems featuring more massive planets together with Earth-like ones tidally interacting with the host-star, tidal migration and heating become dominant factors that must be modelled alongside atmospheric erosion.

For the evolution of the stellar surface rotation rate, we assumed that the star exhibits solid body rotation. This hypothesis appears to be reasonable in view of the rotation profile deduced for the Sun from helioseismic studies (García et al. 2007; Eggenberger, Buldgen, and Salmon 2019), seismic analyses of solar-like MS stars using *Kepler* data (Nielsen et al. 2015; Benomar et al. 2015, 2018) and γDor stars (Saio et al. 2021). While internal differential rotation is fundamental for the dynamo mechanism (as discussed in Section 1), observational evidence from asteroseismology suggests that angular momentum transport is efficient enough to minimize strong radial differential rotation in solar-like stars on main-sequence evolutionary timescales (e.g. Benomar et al. 2015). Therefore, for the purpose of computing the long-term torque and braking history in the SPI code, a solid-body approximation provides a robust and computationally feasible estimate.

The braking at the stellar surface due to magnetized winds is modelled by following the prescription of Matt et al. (2015, 2019), where we calibrated the braking constant $T_\odot = 8 \times 10^{30}$ erg and the coefficient $p = 2.1$ to reproduce the surface rotation of the Sun at the solar age. To account for the distribution of surface rotation rates observed for stars in open clusters and stellar associations (Gallet and Bouvier 2015), we generally consider three values of the initial surface rotation rate on the PMS, calibrated on observational data from Gallet and Bouvier (2015) to reproduce the 25th ($\Omega_{\rm in} = 3.2\ \Omega_\odot$), 50th ($\Omega_{\rm in} = 5\ \Omega_\odot$), and 90th ($\Omega_{\rm in} = 18\ \Omega_\odot$) rotational percentiles (corresponding to fast, moderate, and slow rotating cases), with disk-locking timescales of two and six Myr for the fast and moderate-slow rotators cases, respectively (Eggenberger, Buldgen, and Salmon 2019).

In the following, we describe the fundamental physical ingredients included in the treatment of tidal and radiative interactions, while for a more detailed illustration we refer the interested reader to Privitera et al. (2016), Rao et al. (2018, 2021), Pezzotti et al. (2021, 2025).

4.1. Tidal Interaction

In the SPI code, we consider the equilibrium and dynamical tides dissipated within the host star convective envelope, which can lead to the migration of the planet by means of the angular momentum transferred from the planetary orbit to the stellar surface (or vice versa). Assuming that the planet is on a circular, coplanar orbit around the host star, the net change of its orbital distance is given by:

$$\left(\frac{\dot{a}}{a}\right) = -\frac{\dot{m}_{\rm pl}}{M_{\rm pl} + M_\star} + \left(\frac{\dot{a}}{a}\right)_{\rm eq} + \left(\frac{\dot{a}}{a}\right)_{\rm dyn}, \tag{4}$$

where a is the orbital distance, M_{pl} and $M_\star$ are the planetary and stellar mass, and the dotted quantities are the derivatives with respect to time. The first term in Eq. 4 indicates the change in planetary mass due to photoevaporation (see Section 4.2), assuming that it is lost in space and does not contribute to the exchange of angular momentum between the star and the planetary orbit. The last two terms refer to the contribution of equilibrium and dynamical tides, respectively.

The orbital change due to the equilibrium tide term is computed by following the formalism of Zahn (1966, 1977), as in Privitera et al. (2016):

$$\left(\frac{\dot{a}}{a}\right)_{\rm eq} = \frac{f}{\tau}\frac{M_{\rm env}}{M_\star} q(1+q)\left(\frac{R_\star}{a}\right)^8 \left(\frac{\Omega}{\omega_{\rm pl}} - 1\right), \tag{5}$$

where $M_{\rm env}$ is the mass contained in the stellar convective envelope, q is the ratio between the planetary and the stellar mass, Ω is the surface-rotation rate of the host star, $\omega_{\rm pl}$ is the orbital frequency, and $R_\star$ is the stellar radius. The term τ is the convective turnover timescale, computed as in Rasio et al. (1996), Villaver and Livio (2009):

$$\tau = \left(\frac{M_{\rm env} \left(R_\star - R_{\rm b}\right)^2}{3 L_\star} \right)^{1/3} . \tag{6}$$

where $R_{\rm b}$ is the radius at the bottom of the convective envelope and $L_\star$ is the bolometric luminosity of the host star. The term f in Eq. 5 is a numerical factor obtained from integrating the viscous dissipation of the tidal energy across the convective zone (Villaver and Livio 2009), which is $f = (P_{\rm orb}/2\tau)^2$ (Goldreich and Nicholson 1977) when $\tau < P_{\rm orb}/2$, otherwise $f = 1$.

We account for the impact of dynamical tides in convective envelopes in the form of a frequency-averaged tidal dissipation of inertial waves (Ogilvie 2013; Mathis 2015; Bolmont and Mathis 2016). In particular, we assume a two-layer model (core-envelope), each characterized by a uniform density (Mathis 2015). If the planet is on a circular-coplanar orbit, dynamical tides are active whenever $\omega_{\rm pl} < 2\Omega$ (Ogilvie and Lin 2007). The equation describing the contribution of this type of tides on the evolution of the planetary orbital distance reads as

$$\left(\dot{a}/a\right)_{\rm dyn} = \left(\frac{9}{2 Q'_{\rm d}} \right) q \omega_{\rm pl} \left(\frac{R_\star}{a} \right)^5 \frac{(\Omega - \omega_{\rm pl})}{\mid \Omega - \omega_{\rm pl} \mid}, \tag{7}$$

with $Q'_{\rm d} = 3/(2D_\omega)$ (modified tidal dissipation factor) and $D_\omega = D_{0\omega} D_{1\omega} D_{2\omega}^{-2}$. The 'D' terms are defined as follows:

$$\begin{cases} D_{0\omega} = \dfrac{100\pi}{63} \epsilon^2 \dfrac{\alpha^5}{1-\alpha^5} (1-\gamma)^2, \\ D_{1\omega} = (1-\alpha)^4 \left(1 + 2\alpha + 3\alpha^2 + \frac{3}{2}\alpha^3\right)^2, \\ D_{2\omega} = 1 + \frac{3}{2}\gamma + \frac{5}{2\gamma}\left(1 + \frac{\gamma}{2} - \frac{3\gamma^2}{2}\right)\alpha^3 - \frac{9}{4}(1-\gamma)\alpha^5, \end{cases} \tag{8}$$

where $\alpha = R_{\rm b}/R_\star$, $\beta = M_{\rm b}/M_\star$, $\gamma = \dfrac{\alpha^3(1-\beta)}{\beta(1-\alpha^3)}$, and $\epsilon = \Omega/\sqrt{G M_\star / R_\star^3}$. The term M_b is the mass of the radiative core, considered as the region of the star below the base of the convective envelope. The term D_ω is the frequency-averaged tidal dissipation (Ogilvie 2013). We notice that assuming this schematic stratification for the stellar structure, together with the use of a frequency-averaged dissipation rate for the dynamical tide, adds a certain degree of uncertainty to our results. Nevertheless, while this approach suffers from some schematic simplifications, it has the advantage of providing us with relevant orders of magnitude of tidal dissipation rates accounting for the evolution of the structural and rotational parameters of the host star (Mathis 2015; Bolmont and Mathis 2016; Rao et al. 2018; Barker 2020).

In general, for the formalism treated above, tides widen (respectively shrink) the planetary orbit when it is beyond (respectively inside) the corotation radius, which is defined as the distance at which the orbital and host star rotational periods are equal, namely:

$$a_{\rm cor} = \left[G \left(M_\star + M_{\rm pl} \right) / \Omega^2 \right]^{\frac{1}{3}} . \tag{9}$$

Here, G is the universal gravitational constant. Concerning the formalism used in this work for dynamical tides in the stellar convective envelope, these are efficiently excited in the

form of inertial waves when the planetary orbital distance is larger than a minimum critical value, which is defined as $a_{\rm min} = 4^{-\frac{1}{3}} \times a_{\rm cor}$ (Ogilvie and Lin 2007).

4.2. Radiative Interaction

Exoplanets get irradiated by their host stars since the earliest stages of formation in the protoplanetary disc. This radiative interaction drives the thermal, chemical, and physical evolution of their atmospheres, including escape processes. Several studies on atmospheric evolution have suggested that, after the protoplanetary disc dispersal, during the first $\approx$ 10 – 100 Myr of evolution, the mass loss from primordial hydrogen-rich atmospheres arises as a hydrodynamic outflow, driven by stellar high-energy radiation (X-ray and EUV luminosity) and/or powered by the planetary thermal energy (Kubyshkina 2024, and references therein). Depending on the structural and orbital properties, planets may or may not be able to preserve a fraction of their primordial atmospheres. Close-in ($P_{\rm orb} \lesssim 100$ days), low-mass planets ($M_{\rm pl} \lesssim 10\ M_{\oplus}$) are typically prone to lose the entirety of their primordial atmospheres, while low- to intermediate-mass ones ($10 \lesssim M_{\rm pl}/M_{\oplus} \lesssim 100$) may retain a fraction of it. In this circumstance, the subsequent mass loss on gigayear timescales can be dominated by XUV-driven hydrodynamic escape (Kubyshkina 2024). In contrast, the mass loss from cooler and/or heavier planets, is potentially dominated by kinetic-thermal and non-thermal processes (Kubyshkina 2024).

With our approach, we can investigate the past evolution of star-planet systems determining the conditions for which planets retain a fraction of the primordial hydrogen-rich atmosphere at the stellar age.

To account for the escape of planetary atmospheres in an evolutionary context, in an accurate and computationally feasible way at the same time, we implement the interpolation routine proposed in Kubyshkina and Fossati (2021), based on a dense grid of 1D upper atmosphere hydrodynamic models, which consists of 10235 points with planetary masses from one to 109 $M_{\oplus}$, stellar host masses from 0.4 to 1.3 $M_{\odot}$, and pure hydrogen atmospheric composition (Kubyshkina et al. 2018; Kubyshkina 2024). At each time-step, this routine takes the stellar EUV flux, total planetary radius and orbital distance as input. For the computation of the stellar EUV, we firstly determine the host star X-ray luminosity, for each rotational history, by implementing calibrated formulae linking $R_x - {\rm Ro}$, where R_x is the ratio between the X-ray and bolometric luminosity of the star, while Ro is the Rossby number, as indicated above. In Pezzotti et al. (2021) we presented recalibrated $R_x - {\rm Ro}$ relationships from the works of Wright et al. (2011) and Johnstone, Bartel, and Güdel (2021), according to our computation of the convective turnover timescale (Rasio et al. 1996; Villaver and Livio 2009; Cranmer and Saar 2011). Another method included in our SPI to determine the stellar X-ray luminosity is the one of Jackson, Davis, and Wheatley (2012), that links R_x directly with the stellar age. From the X-ray luminosity it is possible to derive the EUV one from scaling relations proposed in the works of Sanz-Forcada et al. (2011), King et al. (2018), Johnstone, Bartel, and Güdel (2021). For what concerns the evolution of the planetary radius, in the SPI code it is possible to set the planetary core mass and initial fraction of gaseous envelope as input, from which a global radius is determined by means of the fitting formulae from Lopez and Fortney (2014), Chen and Rogers (2016), Otegi, Bouchy, and Helled (2020), depending on the type of planet under study. At each timestep, with the evolution of the planetary mass, the radius is recomputed according to these formulae. Finally, the orbital distance is also evaluated at each time-step, accounting for its potential evolution due to the tidal interaction.

As comprehensively discussed in Kubyshkina et al. (2018), Kubyshkina and Fossati (2021), the implementation of this method allows one to extract quickly and efficiently mass loss rates for a certain asset of star-planet systems from a broad grid of models, enabling the use of accurate results in planetary evolution calculations. With this approach, we avoid the use of much more approximate formulae, as in the case of the energy-limited one, which has been proven to significantly underestimate the atmospheric escape in young and/or low-gravity planets, and to overestimate it for high-gravity ones. At the same time, it is fundamental to recall that a study of the atmospheric escape properties relative to a specific snapshot of the star-planet system requires a dedicated consideration of the planetary atmospheric chemical composition, thermodynamic structure, together with the host star short term activity and flaring (e.g. Gronoff et al. 2020, for a detailed review on the topic).

5. Results and Discussion

We applied our integrated framework to the Solar Standard Model defined in Section 1 to reconstruct the rotational and magnetic history of the Sun. By coupling the structural evolution computed with CLES to the orbital and angular momentum evolution in the SPI code, we derived the evolution of the surface rotation rate (Ω) and X-ray luminosity (L_x) from the protoplanetary disc dispersal to the current solar age.

5.1. Rotational Evolution and Magnetic Braking

In Figure 3 we show an example of the evolution of the surface rotation rate and X-ray luminosity as function of time for a 1 $M_\odot$ star computed with the SPI code from the dispersal of the planetary disk to the TAMS, considering the three different initial rotation rates: slow ($\Omega_{in} = 3.2\ \Omega_\odot$), moderate ($\Omega_{in} = 5\ \Omega_\odot$), and fast ($\Omega_{in} = 18\ \Omega_\odot$) rotation (Eggenberger, Buldgen, and Salmon 2019; Gallet and Bouvier 2015).

The comparison between calculated and observed surface angular velocity shows that in the case of the Sun-Earth system, different initial rotational conditions are important only in the PMS phases. As a consequence, it is not possible to determine the initial rotational conditions of the Sun from its present rotation rate. By comparing the tracks shown in the middle and bottom panels of Figure 3, it is possible to notice that while with the recalibration of the Johnstone, Bartel, and Güdel (2021) the tracks tend to overpredict the observed X-ray luminosity of the Sun, with the recalibration of Wright et al. (2011) we obtain a better agreement.

In Figure 4, we show an example of the evolution of the atmospheric mass and total radius for a planet at 1 AU, with initial core mass 1 $M_\oplus$, topped by a H-He rich atmosphere with initial mass 0.25 $M_\oplus$, under the impact of the host star XUV flux, for initial surface rotation rates $\Omega_{in} = 3.2\ \Omega_\odot$ and $\Omega_{in} = 18\ \Omega_\odot$. For the computation of the planetary radius we applied the formulae from Lopez and Fortney (2014), while for the planetary mass loss we used the analytic formulae from Kubyshkina et al. (2018).

This result highlights a fundamental degeneracy: for a star of the solar mass and age, the current rotation rate does not retain memory of the initial conditions. The observational evidence on the distribution of surface rotation rates for solar-like stars in open clusters and stellar associations (Gallet and Bouvier 2015) shows that this distribution becomes significantly narrower for stars at evolutionary stages similar or more advanced than the one of the Sun. Thanks to the action of the magnetic braking, independently from the initial surface

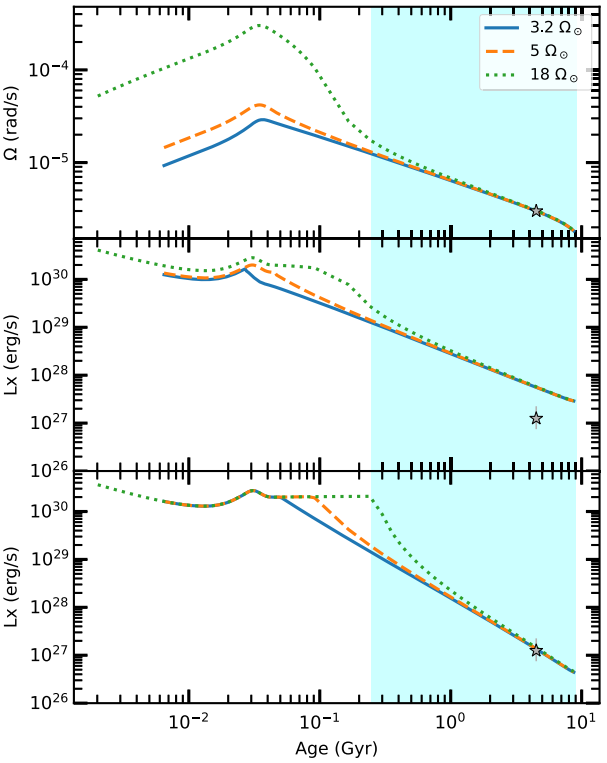

Figure 3 Evolution of the surface rotation rate Ω (top) and theoretical X-ray luminosity L_X (middle and bottom) for a 1 $M_\odot$ model. Tracks correspond to fast (blue solid), moderate (orange dashed), and slow (green dotted) initial rotation. Top panel: the star symbol indicates the surface rotation rate of the Sun at solar age $\Omega_\odot = 2.9 \times 10^{-6}$rad/s. Middle panel: L_X computed following Johnstone, Bartel, and Güdel (2021). Bottom panel: L_X computed following Wright et al. (2011). The star symbol in the middle and bottom panels indicates the average observed solar L_X, with error bars representing the magnetic cycle variation (Judge, Solomon, and Ayres 2003). The light-blue region highlights the main sequence phase of the evolution.

rotation rate harboured by the star at the unlocking from the protostellar disk, during the MS the surface rotation rate evolves with respect to the age as $\Omega \propto t^{-1/2}$ (Skumanich 1972).

However, the early rotational history strongly affects XUV irradiation: a fast-rotating young Sun would have irradiated the early Earth to a significantly higher cumulative XUV flux compared to a slow-rotating scenario. This difference in the first ≈500 Myr is critical for the survival of the primordial planetary atmosphere, as the hydrodynamic escape rates are most severe during these early active phases (see Figure 4).

5.2. Constraining the X-ray History

The evolution of the stellar X-ray luminosity is shown in the middle and bottom panels of Figure 3. In these panels, we compare the X-ray tracks obtained by using two different recalibrations of the activity-rotation relationship (R_x − Ro). When employing the recalibration of the Johnstone, Bartel, and Güdel (2021) relations (middle panel) and developed in Pezzotti et al. (2021), our models tend to overpredict the observed X-ray luminosity of the current Sun. Conversely, utilizing the recalibration based on Wright et al. (2011) (bottom panel) yields a better agreement with the observed average solar X-ray emission and its variation over a magnetic cycle ($\log L_X \approx 26.7-27.3$) (Judge, Solomon, and Ayres 2003).

Understanding how the average X-ray irradiation of low-mass solar-like stars varies as a function of age, surface rotation, and Rossby number is very challenging. A comprehensive investigation on the functioning and evolution of magnetic activity would require knowledge of stellar fundamental properties (age, mass, radius, metallicity, etc), rotation features,

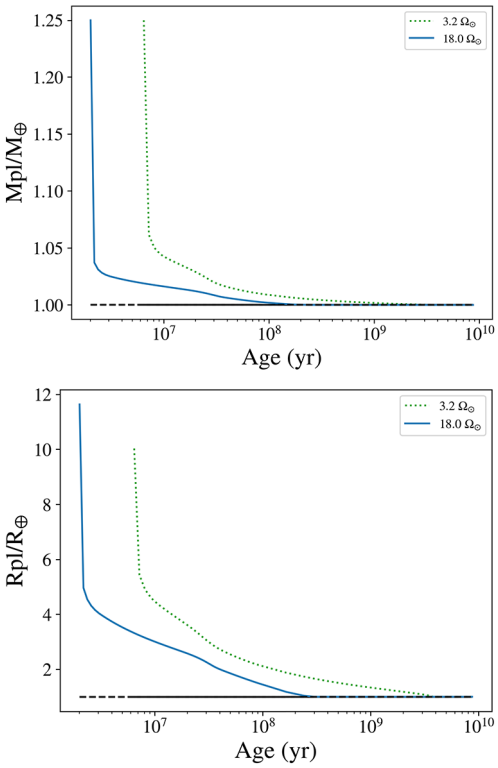

Figure 4 Evolution of the atmospheric mass (top) for a planet at 1 AU, with initial core mass 1 $M_{\oplus}$ and initial atmospheric mass fraction $f = 20\%$. The green-dotted and blue-solid lines show the evolution computed for a host star with initial surface rotation rate $\Omega_{\rm in} = 18\ \Omega_{\odot}$ and $\Omega_{\rm in} = 3.2\ \Omega_{\odot}$, respectively. The black-dashed line indicates the mass of the core. Evolution of the total planetary radius (bottom). The black-dashed line indicates the radius of the planetary core.

and magnetic activity proxies (e.g. X-ray luminosity) with high accuracy, for a statistically significant number of stars.

Thanks to the advent of space-based photometry, asteroseismology is playing a crucial role in determining fundamental parameters for an increasing number of low-mass and solar-like stars. In a recent work, Pezzotti et al. (2026) revisited the magnetic activity-rotation-age relationships including the largest sample of stars with highest quality asteroseismic data from now to the launch of PLATO (*Kepler* Legacy sample), selecting the ones for which surface rotation and X-ray detections are available. Thanks to this work, a recalibration of the most popular activity-age and activity-rotation relationships in the literature was performed, accounting for precise fundamental parameters. Nevertheless, as highlighted in Pezzotti et al. (2026), a statistically more significant number of well- and comprehensively-characterised stars is needed to perform accurate calibrations and potentially disentangle diverse regimes in the magnetic activity across the evolution of stars (e.g. variation of activity for weakened magnetic braking). Therefore, joining accurate stellar characterisation through asteroseismology, to magnetic activity and star-planet interaction studies is crucial to increase the sample of stars with properties analogous to the ones of the Sun, and investigate the evolution and impact of their activity across a planetary system lifetime.

6. Conclusion

While the concept of habitability has been discussed in the literature for some decades, it is only recently that complementary observational and theoretical techniques have been suc-

cessfully implemented to obtain a significant advancement in exoplanetary characterization and in order to understand how long an exoplanet may maintain habitability, so that life can have the opportunity to originate and to develop (e.g. Hu et al. 2024; Rukdee 2024; Tinetti et al. 2016).

In this work, we have presented a comprehensive strategy to characterize star-planet interactions by treating the Sun as a "Rosetta Stone": we have adapted and applied different techniques to interpret phenomena detected in remote exoplanetary systems by drawing parallels with the Sun-Earth system. Our strategy combines use of accurate asteroseismic ages, Ca II H and K proxies for stellar wind pressure and theoretical modelling to determine parameters of exoplanets orbiting around solar-like stars and to investigate how stellar radiation, gravitational-tidal and magnetic activity influence the climate long-term variability. The procedure allows us to estimate how long an H/He rich atmosphere could resist to the action of stellar wind and the XUV flux quantifying the portion of the atmosphere which could potentially be eroded.

We plan to apply the method to a large sample of main sequence solar-like G type stars observed by TESS and *Kepler*, with mass $M = 0.8-1.2\ M_{\odot}$, with a photospheric temperature of 5000–6000 K, and a similar activity regime of the Sun for which asteroseismic, spectroscopic, and photometric observations have been already detected and released. The results will be of relevance especially in the context of the future PLATO (PLAnetary Transits and Oscillations of stars) (Rauer et al. 2014) space mission, whose primary goal will be to detect terrestrial exoplanets in the habitable zone of Sun-like stars.

Although the present work focuses on Sun–Earth analogues, one should be aware that many known exoplanets orbit stars of different masses, rotation rates, and activity levels. By moving beyond solar-like stars, it will be possible to map the habitability landscape of a broader sample of stars. In fact, extending the present framework to rapidly rotating young solar analogues, active K dwarfs, and M dwarfs hosting terrestrial planets would allow to infer the impact of stronger stellar winds, higher XUV fluxes, and different magnetic topologies on planetary climates to be assessed. These regimes, observationally more challenging, represent critical conditions of atmospheric erosion and habitability boundaries.

In particular, it is interesting to mention the case of M-type stars, which are the most abundant stellar population in the Galaxy, characterized by low masses $\approx (0.1-0.6)\ M_{\odot}$ and low effective temperatures $T_{\rm eff} < 4000$ K. These stars are convective throughout their interiors, which theoretically should support the presence of solar-like oscillations driven by turbulent convection. However, the detection of such oscillations in M dwarfs has proven challenging due to their low luminosities and the small amplitudes of the oscillations (Rodríguez-López 2019). Despite reaching detection limits below ten μmag for the brightest objects, no definitive detections were made in the M dwarf sample analysed by Rodríguez et al. (2016). Nevertheless, future plans are to include testing the method to stellar types and activity regimes beyond the Sun–Earth case and to planets on closer-in orbits where tidal locking, intense irradiation, and stronger magnetic interactions dominate. These extensions will require most probably coupling the present approach with 3D MHD stellar wind simulations and more sophisticated atmospheric escape models.

Acknowledgments The authors thank the referee for their careful reading of the manuscript and their constructive suggestions.

Author Contributions MPDM is responsible of the entire manuscript and in particular she takes care of the use of asteroseismic tools and determination of stellar/solar parameters including the inversion results. CP is responsible of the tidal and radiative star-planet modelling interactions in exoplanetary systems. RR takes care

of the analysis of the solar magnetic activity and the analysis of the solar-wind-magnetosphere interaction. NM is expert of stellar evolution modelling and production of figures. LG takes care of the analysis of the solar magnetic activity and the analysis of the solar-wind-magnetosphere interaction.

Funding Information Open access funding provided by Istituto Nazionale di Astrofisica within the CRUI-CARE Agreement. The authors wish to acknowledge funding received by the Italian Space Agency and the Ministry of University and Research through 'Space It up' Spoke 6. CP thanks the Belgian Federal Science Policy Office (BELSPO) for the financial support in the framework of the PRODEX (Program of the European Space Agency) (ESA) under contract number 4000141194. The authors acknowledge funding for the position of NM from the research theory grant "Synergic tools for characterizing solar-like stars and habitability conditions of exoplanets" (PI MP Di Mauro) under the INAF national call for Fundamental Research 2023.

Data Availability No datasets were generated or analysed during the current study.

Declarations

Competing Interests The authors declare no competing interests.

Open Access This article is licensed under a Creative Commons Attribution 4.0 International License, which permits use, sharing, adaptation, distribution and reproduction in any medium or format, as long as you give appropriate credit to the original author(s) and the source, provide a link to the Creative Commons licence, and indicate if changes were made. The images or other third party material in this article are included in the article's Creative Commons licence, unless indicated otherwise in a credit line to the material. If material is not included in the article's Creative Commons licence and your intended use is not permitted by statutory regulation or exceeds the permitted use, you will need to obtain permission directly from the copyright holder. To view a copy of this licence, visit http://creativecommons.org/licenses/by/4.0/.

References

Airapetian, V.S., Barnes, R., Cohen, O., Collinson, G.A., Danchi, W.C., Dong, C.F., Del Genio, A.D., France, K., Garcia-Sage, K., Glocer, A., Gopalswamy, N., Grenfell, J.L., Gronoff, G., Güdel, M., Herbst, K., Henning, W.G., Jackman, C.H., Jin, M., Johnstone, C.P., Kaltenegger, L., Kay, C.D., Kobayashi, K., Kuang, W., Li, G., Lynch, B.J., Lüftinger, T., Luhmann, J.G., Maehara, H., Mlynczak, M.G., Notsu, Y., Osten, R.A., Ramirez, R.M., Rugheimer, S., Scheucher, M., Schlieder, J.E., Shibata, K., Sousa-Silva, C., Stamenković, V., Strangeway, R.J., Usmanov, A.V., Vergados, P., Verkhoglyadova, O.P., Vidotto, A.A., Voytek, M., Way, M.J., Zank, G.P., Yamashiki, Y.: 2020, Impact of space weather on climate and habitability of terrestrial-type exoplanets. *Int. J. Astrobiol.* **19**, 136. DOI. ADS.

Alvarado-Gómez, J.D., Hussain, G.A.J., Cohen, O., Drake, J.J., Garraffo, C., Grunhut, J., Gombosi, T.I.: 2016a, Simulating the environment around planet-hosting stars. I. Coronal structure. *Astron. Astrophys.* **588**, A28. DOI. ADS.

Alvarado-Gómez, J.D., Hussain, G.A.J., Cohen, O., Drake, J.J., Garraffo, C., Grunhut, J., Gombosi, T.I.: 2016b, Simulating the environment around planet-hosting stars. II. Stellar winds and inner astrospheres. *Astron. Astrophys.* **594**, A95. DOI. ADS.

Barker, A.J.: 2020, Tidal dissipation in evolving low-mass and solar-type stars with predictions for planetary orbital decay. *Mon. Not. R. Astron. Soc.* **498**, 2270. DOI. ADS.

Basu, S., Antia, H.M.: 1997, Seismology of the base of the solar convection zone. *Mon. Not. R. Astron. Soc.* **287**, 189. DOI. ADS

Baum, A.C., Wright, J.T., Luhn, J.K., Isaacson, H.: 2022, Five decades of chromospheric activity in 59 Sun-like stars and new Maunder minimum candidate HD 166620. *Astron. J.* **163**, 183. DOI. ADS.

Benomar, O., Takata, M., Shibahashi, H., Ceillier, T., García, R.A.: 2015, Nearly uniform internal rotation of solar-like main-sequence stars revealed by space-based asteroseismology and spectroscopic measurements. *Mon. Not. R. Astron. Soc.* **452**, 2654. DOI. ADS.

Benomar, O., Bazot, M., Nielsen, M.B., Gizon, L., Sekii, T., Takata, M., Hotta, H., Hanasoge, S., Sreenivasan, K.R., Christensen-Dalsgaard, J.: 2018, Asteroseismic detection of latitudinal differential rotation in 13 Sun-like stars. *Science* **361**, 1231. DOI. ADS.

Böhm-Vitense, E.: 1958, Über die Wasserstoffkonvektionszone in Sternen verschiedener Effektivtemperaturen und Leuchtkräfte. Mit 5 Textabbildungen. *Z. Astrophys.* **46**, 108. ADS.

Bolmont, E., Mathis, S.: 2016, Effect of the rotation and tidal dissipation history of stars on the evolution of close-in planets. *Celest. Mech. Dyn. Astron.* **126**, 275. DOI. ADS.

Brun, A.S., Browning, M.K.: 2017, Magnetism, dynamo action and the solar-stellar connection. *Living Rev. Sol. Phys.* **14**, 4. DOI. ADS.

Charbonneau, P.: 2020, Dynamo models of the solar cycle. *Living Rev. Sol. Phys.* **17**, 4. DOI. ADS.

Chebly, J.J., Alvarado-Gómez, J.D., Poppenhäger, K., Garraffo, C.: 2023, Numerical quantification of the wind properties of cool main sequence stars. *Mon. Not. R. Astron. Soc.* **524**, 5060. DOI. ADS.

Chen, H., Rogers, L.A.: 2016, Evolutionary analysis of gaseous sub-Neptune-mass planets with MESA. *Astrophys. J.* **831**, 180. DOI. ADS.

Corsaro, E., Bonanno, A., Mathur, S., García, R.A., Santos, A.R.G., Breton, S.N., Khalatyan, A.: 2021, A calibration of the Rossby number from asteroseismology. *Astron. Astrophys.* **652**, L2. DOI. ADS.

Cranmer, S.R., Saar, S.H.: 2011, Testing a predictive theoretical model for the mass loss rates of cool stars. *Astrophys. J.* **741**, 54. DOI. ADS.

Deheuvels, S., Doğan, G., Goupil, M.J., Appourchaux, T., Benomar, O., Bruntt, H., Campante, T.L., Casagrande, L., Ceillier, T., Davies, G.R., De Cat, P., Fu, J.N., García, R.A., Lobel, A., Mosser, B., Reese, D.R., Regulo, C., Schou, J., Stahn, T., Thygesen, A.O., Yang, X.H., Chaplin, W.J., Christensen-Dalsgaard, J., Eggenberger, P., Gizon, L., Mathis, S., Molenda-Żakowicz, J., Pinsonneault, M.: 2014, Seismic constraints on the radial dependence of the internal rotation profiles of six *Kepler* subgiants and young red giants. *Astron. Astrophys.* **564**, A27. DOI. ADS.

Di Mauro, M.P., Dziembowski, W.A., Paternó, L.: 1998, Rotation of the solar interior: new results by helioseismic data inversions. In: Korzennik, S. (ed.) *Structure and Dynamics of the Interior of the Sun and Sun-Like Stars*, *ESA Special Publication* **418**, 759. ADS.

Di Mauro, M.P., Ventura, R., Corsaro, E., Lustosa De Moura, B.: 2018, The rotational shear layer inside the early red-giant star KIC 4448777. *Astrophys. J.* **862**, 9. DOI. ADS.

Dungey, J.W.: 1961, Interplanetary magnetic field and the auroral zones. *Phys. Rev. Lett.* **6**, 47. DOI. ADS.

Eggenberger, P., Buldgen, G., Salmon, S.J.A.J.: 2019, Rotation rate of the solar core as a key constraint to magnetic angular momentum transport in stellar interiors. *Astron. Astrophys.* **626**, L1. DOI. ADS.

Eyelade, A.V., Stepanova, M., Espinoza, C.M., Antonova, E.E., Kirpichev, I.P.: 2024, The response of the Earth magnetosphere to changes in the solar wind dynamic pressure: 1. Plasma and magnetic pressures. *J. Geophys. Res. Space Phys.* **129**, e2023JA031948. DOI. ADS

Gallet, F., Bouvier, J.: 2015, Improved angular momentum evolution model for solar-like stars. II. Exploring the mass dependence. *Astron. Astrophys.* **577**, A98. DOI. ADS.

García, R.A., Turck-Chièze, S., Jiménez-Reyes, S.J., Ballot, J., Pallé, P.L., Eff-Darwich, A., Mathur, S., Provost, J.: 2007, Tracking solar gravity modes: the dynamics of the solar core. *Science* **316**, 1591. DOI. ADS.

Garraffo, C., Drake, J.J., Cohen, O.: 2016, The space weather of Proxima Centauri b. *Astrophys. J. Lett.* **833**, L4. DOI. ADS.

Garraffo, C., Drake, J.J., Dotter, A., Choi, J., Burke, D.J., Moschou, S.P., Alvarado-Gómez, J.D., Kashyap, V.L., Cohen, O.: 2018, The revolution revolution: magnetic morphology driven spin-down. *Astrophys. J.* **862**, 90. DOI. ADS.

Garraffo, C., Alvarado-Gómez, J.D., Cohen, O., Drake, J.J.: 2022, Revisiting the space weather environment of Proxima Centauri b. *Astrophys. J. Lett.* **941**, L8. DOI. ADS.

Goldreich, P., Nicholson, P.D.: 1977, Turbulent viscosity and Jupiter's tidal Q. *Icarus* **30**, 301. DOI. ADS.

Grießmeier, J.-M., Stadelmann, A., Penz, T., Lammer, H., Selsis, F., Ribas, I., Guinan, E.F., Motschmann, U., Biernat, H.K., Weiss, W.W.: 2004, The effect of tidal locking on the magnetospheric and atmospheric evolution of "Hot Jupiters". *Astron. Astrophys.* **425**, 753. DOI. ADS.

Gronoff, G., Arras, P., Baraka, S., Bell, J.M., Cessateur, G., Cohen, O., Curry, S.M., Drake, J.J., Elrod, M., Erwin, J., Garcia-Sage, K., Garraffo, C., Glocer, A., Heavens, N.G., Lovato, K., Maggiolo, R., Parkinson, C.D., Simon Wedlund, C., Weimer, D.R., Moore, W.B.: 2020, Atmospheric escape processes and planetary atmospheric evolution. *J. Geophys. Res. Space Phys.* **125**, e27639. DOI. ADS.

Hall, J.C., Lockwood, G.W.: 1995, The solar-stellar spectrograph: project description, data calibration, and initial results. *Astrophys. J.* **438**, 404. DOI. ADS.

Hall, J.C., Lockwood, G.W.: 2004, The chromospheric activity and variability of cycling and flat activity solar-analog stars. *Astrophys. J.* **614**, 942. DOI. ADS.

Hu, R., Bello-Arufe, A., Zhang, M., Paragas, K., Zilinskas, M., van Buchem, C., Bess, M., Patel, J., Ito, Y., Damiano, M., Scheucher, M., Oza, A.V., Knutson, H.A., Miguel, Y., Dragomir, D., Brandeker, A., Demory, B.-O.: 2024, A secondary atmosphere on the rocky exoplanet 55 Cancri e. *Nature* **630**, 609. DOI. ADS.

Jackson, A.P., Davis, T.A., Wheatley, P.J.: 2012, The coronal X-ray-age relation and its implications for the evaporation of exoplanets. *Mon. Not. R. Astron. Soc.* **422**, 2024. DOI. ADS.

Jao, W.-C., Couperus, A.A., Vrijmoet, E.H., Wright, N.J., Henry, T.J.: 2022, Estimating the convective turnover time. *Astrophys. J.* **940**, 145. DOI. ADS

Johnstone, C.P., Bartel, M., Güdel, M.: 2021, The active lives of stars: a complete description of the rotation and XUV evolution of F, G, K, and M dwarfs. *Astron. Astrophys.* **649**, A96. DOI. ADS.

Judge, P.G., Solomon, S.C., Ayres, T.R.: 2003, An estimate of the sun's ROSAT-PSPC X-ray luminosities using SNOE-SXP measurements. *Astrophys. J.* **593**, 534. DOI. ADS.

King, G.W., Wheatley, P.J., Salz, M., Bourrier, V., Czesla, S., Ehrenreich, D., Kirk, J., Lecavelier des Etangs, A., Louden, T., Schmitt, J., Schneider, P.C.: 2018, The XUV environments of exoplanets from Jupiter-size to super-Earth. *Mon. Not. R. Astron. Soc.* **478**, 1193. DOI. ADS.

Kubyshkina, D.: 2024, Planetary atmospheres Through Time: Effects of Mass Loss and Thermal Evolution. arXiv e-prints. arXiv. DOI. ADS.

Kubyshkina, D.I., Fossati, L.: 2021, Extending a grid of hydrodynamic planetary upper atmosphere models. *Res. Notes Amer. Astron. Soc.* **5**, 74. DOI. ADS.

Kubyshkina, D., Fossati, L., Erkaev, N.V., Cubillos, P.E., Johnstone, C.P., Kislyakova, K.G., Lammer, H., Lendl, M., Odert, P.: 2018, Overcoming the limitations of the energy-limited approximation for planet atmospheric escape. *Astrophys. J. Lett.* **866**, L18. DOI. ADS.

Landin, N.R., Mendes, L.T.S., Vaz, L.P.R.: 2010, Theoretical values of convective turnover times and Rossby numbers for solar-like, pre-main sequence stars. *Astron. Astrophys.* **510**, A46. DOI. ADS.

Larmor, J.: 1919, How could a rotating body such as the Sun become a magnet? *Rep. Br. Assoc.* **87**, 159.

Lebreton, Y., Goupil, M.J.: 2014, Asteroseismology for 'a la carte' stellar age-dating and weighing. Age and mass of the CoRoT exoplanet host HD 52265 *Astron. Astrophys.* **569**, 21L. DOI ADS.

Lopez, E.D., Fortney, J.J.: 2014, Understanding the mass-radius relation for sub-Neptunes: radius as a proxy for composition. *Astrophys. J.* **792**, 1. DOI. ADS.

Lundkvist, M.S., Huber, D., Aguirre, V.S., Chaplin, W.J.: 2018, Characterizing host stars using asteroseismology. In: Deeg, H.J., Belmonte, J.A. (eds.) *Handbook of Exoplanets* **177**. DOI. ADS.

Magic, Z., Weiss, A., Asplund, M.: 2015, The Stagger-grid: a grid of 3D stellar atmosphere models. III. The relation to mixing-length convection theory. *Astron. Astrophys.* **573**, A90. DOI. ADS.

Mathis, S.: 2015, Variation of tidal dissipation in the convective envelope of low-mass stars along their evolution. *Astron. Astrophys.* **580**, L3. DOI. ADS.

Mathur, S., García, R.A., Ballot, J., et al.: 2014, Magnetic activity of F stars observed by *Kepler*. *Astron. Astrophys.* **562**, A124. DOI. ADS.

Matt, S.P., Brun, A.S., Baraffe, I., Bouvier, J., Chabrier, G.: 2015, The mass-dependence of angular momentum evolution in Sun-like stars. *Astrophys. J. Lett.* **799**, L23. DOI. ADS.

Matt, S.P., Brun, A.S., Baraffe, I., Bouvier, J., Chabrier, G.: 2019, Erratum: "The mass-dependence of angular momentum evolution in Sun-like stars". *Astrophys. J. Lett.* **870**, L27. DOI. ADS.

Metcalfe, T.S., Corsaro, E., Bonanno, A., Creevey, O.L., van Saders, J.L.: 2024, Extending the asteroseismic calibration of the stellar Rossby number. *Res. Notes Amer. Astron. Soc.* **8**, 260. DOI. ADS.

Miglio, A., Chiappini, C., Mosser, B., Morel, T., Barbieri, M., Girardi, L., Montalbán, J., Noels, A., Valentini, M., Bossini, D., et al.: 2017, PLATO as it is : A legacy mission for Galactic archaeology. *Astronomische Nachrichten* **6**, 644. DOI. ADS.

Mosser, B., Goupil, M.J., Belkacem, K., Marques, J.P., Beck, P.G., Bloemen, S., De Ridder, J., Barban, C., Deheuvels, S., Elsworth, Y., Hekker, S., Kallinger, T., Ouazzani, R.M., Pinsonneault, M., Samadi, R., Stello, D., García, R.A., Klaus, T.C., Li, J., Mathur, S., Morris, R.L.: 2012, Spin down of the core rotation in red giants. *Astron. Astrophys.* **548**, A10. DOI. ADS.

Nielsen, M.B., Schunker, H., Gizon, L., Ball, W.H.: 2015, Constraining differential rotation of Sun-like stars from asteroseismic and starspot rotation periods. *Astron. Astrophys.* **582**, A10. DOI. ADS.

Nordlund, Å., Stein, R.F., Asplund, M.: 2009, Solar surface convection. *Living Rev. Sol. Phys.* **6**, 2. DOI. ADS.

Noyes, R.W., Hartmann, L.W., Baliunas, S.L., Duncan, D.K., Vaughan, A.H.: 1984, Rotation, convection, and magnetic activity in lower main-sequence stars. *Astrophys. J.* **279**, 763. DOI. ADS

Ogilvie, G.I.: 2013, Tides in rotating barotropic fluid bodies: the contribution of inertial waves and the role of internal structure. *Mon. Not. R. Astron. Soc.* **429**, 613. DOI. ADS.

Ogilvie, G.I., Lin, D.N.C.: 2007, Tidal dissipation in rotating solar-type stars. *Astrophys. J.* **661**, 1180. DOI. ADS.

Otegi, J.F., Bouchy, F., Helled, R.: 2020, Revisited mass-radius relations for exoplanets below 120 $M_{\oplus}$. *Astron. Astrophys.* **634**, A43. DOI. ADS.

Parker, E.N.: 1955, Hydromagnetic dynamo models. *Astrophys. J.* **122**, 293. DOI. ADS.

Parker, E.N.: 1958, Dynamics of the interplanetary gas and magnetic fields. *Astrophys. J.* **128**, 664. DOI. ADS.

Perdelwitz, V., Trifonov, T., Teklu, J.T., Sreenivas, K.R., Tal-Or, L.: 2024, Analysis of the public HARPS/ESO spectroscopic archive. Ca II H&K time series for the HARPS radial velocity database. *Astron. Astrophys.* **683**, A125. DOI. ADS.

Pezzotti, C., Eggenberger, P., Buldgen, G., Meynet, G., Bourrier, V., Mordasini, C.: 2021, Revisiting *Kepler*-444. II. Rotational, orbital, and high-energy fluxes evolution of the system. *Astron. Astrophys.* **650**, A108. DOI. ADS.

Pezzotti, C., Buldgen, G., Magaudda, E., Farnir, M., Van Grootel, V., Bellotti, S., Poppenhaeger, K.: 2025, Planetary inward migration as the potential cause of GJ 504's fast rotation and bright X-ray luminosity: new constraints from eROSITA. *Astron. Astrophys.* **694**, A179. DOI. ADS.

Pezzotti, C., Bétrisey, J., Buldgen, G., Gilfanov, M., Bikmaev, I., Sunyaev, R., Isık, E., Gosset, E., Wright, N.J.: 2026, The stellar activity-rotation-age relationship under the lens of asteroseismology. *Astron. Astrophys.* **706**, A257. DOI. ADS.

Pizzolato, N., Maggio, A., Micela, G., Sciortino, S., Ventura, P.: 2003, The stellar activity-rotation relationship revisited: dependence of saturated and non-saturated X-ray emission regimes on stellar mass for late-type dwarfs. *Astron. Astrophys.* **397**, 147. DOI, ADS,

Pont, F.: 2009, Empirical evidence for tidal evolution in transiting planetary systems. *Mon. Not. R. Astron. Soc.* **396**, 1789. DOI. ADS.

Privitera, G., Meynet, G., Eggenberger, P., Vidotto, A.A., Villaver, E., Bianda, M.: 2016, Star-planet interactions. II. Is planet engulfment the origin of fast rotating red giants? *Astron. Astrophys.* **593**, A128. DOI. ADS.

Rao, S., Meynet, G., Eggenberger, P., Haemmerlé, L., Privitera, G., Georgy, C., Ekström, S., Mordasini, C.: 2018, Star-planet interactions. V. Dynamical and equilibrium tides in convective zones. *Astron. Astrophys.* **618**, A18. DOI. ADS.

Rao, S., Pezzotti, C., Meynet, G., Eggenberger, P., Buldgen, G., Mordasini, C., Bourrier, V., Ekström, S., Georgy, C.: 2021, Star-planet interactions. VI. Tides, stellar activity, and planetary evaporation. *Astron. Astrophys.* **651**, A50. DOI. ADS.

Rasio, F.A., Tout, C.A., Lubow, S.H., Livio, M.: 1996, Tidal decay of close planetary orbits. *Astrophys. J.* **470**, 1187. DOI. ADS.

Rauer, H., Catala, C., Aerts, C., Appourchaux, T., Benz, W., Brandeker, A., Christensen-Dalsgaard, J., Deleuil, M., Gizon, L., Goupil, M.-J., Güdel, M., Janot-Pacheco, E., Mas-Hesse, M., Pagano, I., Piotto, G., Pollacco, D., Santos, C., Smith, A., Suárez, J.-C., Szabó, R., Udry, S., Adibekyan, V., Alibert, Y., Almenara, J.-M., Amaro-Seoane, P., Eiff, A.-v., Asplund, M.M., Antonello, E., Barnes, S., Baudin, F., Belkacem, K., Bergemann, M., Bihain, G., Birch, A.C., Bonfils, X., Boisse, I., Bonomo, A.S., Borsa, F., Brandão, I.M., Brocato, E., Brun, S., Burleigh, M., Burston, R., Cabrera, J., Cassisi, S., Chaplin, W., Charpinet, S., Chiappini, C., Church, R.P., Csizmadia, S., Cunha, M., Damasso, M., Davies, M.B., Deeg, H.J., Díaz, R.F., Dreizler, S., Dreyer, C., Eggenberger, P., Ehrenreich, D., Eigmüller, P., Erikson, A., Farmer, R., Feltzing, S., de Oliveira Fialho, F., Figueira, P., Forveille, T., Fridlund, M., García, R.A., Giommi, P., Giuffrida, G., Godolt, M., Gomes da Silva, J., Granzer, T., Grenfell, J.L., Grotsch-Noels, A., Günther, E., Haswell, C.A., Hatzes, A.P., Hébrard, G., Hekker, S., Helled, R., Heng, K., Jenkins, J.M., Johansen, A., Khodachenko, M.L., Kislyakova, K.G., Kley, W., Kolb, U., Krivova, N., Kupka, F., Lammer, H., Lanza, A.F., Lebreton, Y., Magrin, D., Marcos-Arenal, P., Marrese, P.M., Marques, J.P., Martins, J., Mathis, S., Mathur, S., Messina, S., Miglio, A., Montalban, J., Montalto, M., Monteiro, M.J.P.F.G., Moradi, H., Moravveji, E., Mordasini, C., Morel, T., Mortier, A., Nascimbeni, V., Nelson, R.P., Nielsen, M.B., Noack, L., Norton, A.J., Ofir, A., Oshagh, M., Ouazzani, R.-M., Pápics, P., Parro, V.C., Petit, P., Plez, B., Poretti, E., Quirrenbach, A., Ragazzoni, R., Raimondo, G., Rainer, M., Reese, D.R., Redmer, R., Reffert, S., Rojas-Ayala, B., Roxburgh, I.W., Salmon, S., Santerne, A., Schneider, J., Schou, J., Schuh, S., Schunker, H., Silva-Valio, A., Silvotti, R., Skillen, I., Snellen, I., Sohl, F., Sousa, S.G., Sozzetti, A., Stello, D., Strassmeier, K.G., Švanda, M., Szabó, G.M., Tkachenko, A., Valencia, D., Van Grootel, V., Vauclair, S.D., Ventura, P., Wagner, F.W., Walton, N.A., Weingrill, J., Werner, S.C., Wheatley, P.J., Zwintz, K.: 2014, The PLATO 2.0 mission. *Exp. Astron.* **38**, 249. DOI. ADS.

Reda, R., Di Mauro, M.P., Giovannelli, L., Alberti, T., Berrilli, F., Corsaro, E.: 2022, A synergic strategy to characterize the habitability conditions of exoplanets hosted by solar-type stars. *Front. Astron. Space Sci.* **9**, 909268. DOI. ADS.

Reda, R., Giovannelli, L., Alberti, T., Berrilli, F., Bertello, L., Del Moro, D., Di Mauro, M.P., Giobbi, P., Penza, V.: 2023, The exoplanetary magnetosphere extension in Sun-like stars based on the solar wind – solar UV relation. *Mon. Not. R. Astron. Soc.* **519**, 6088. DOI. ADS.

Reda, R., Stumpo, M., Giovannelli, L., Alberti, T., Consolini, G.: 2024, Disentangling the solar activity-solar wind predictive causality at Space Climate scales. *Rend. Lincei, Sci. Fis. Nat.* **35**, 49. DOI. ADS.

Reinhold, T., Bell, K.J., Kuszlewicz, J., Hekker, S., Shapiro, A.I.: 2019, Transition from spot to faculae domination. An alternate explanation for the dearth of intermediate *Kepler* rotation periods. *Astron. Astrophys.* **621**, A21. DOI. ADS.

Rodríguez, E., Rodríguez-López, C., López-González, M.J., Amado, P.J., Ocando, S., Berdiñas, Z.M.: 2016, Search for pulsations in M dwarfs in the *Kepler* short-cadence data base. *Mon. Not. R. Astron. Soc.* **457**, 1851. DOI. ADS.

Rodríguez-López, C.: 2019, The quest for pulsating M dwarf stars. *Front. Astron. Space Sci.* **6**, 76. DOI. ADS.

Rukdee, S.: 2024, Instrumentation Prospects for Rocky Exoplanet Atmospheres Studies with High Resolution Spectroscopy, *Scientific Reports* **14**, 27356. DOI. ADS.

Saio, H., Takata, M., Lee, U., Li, G., Van Reeth, T.: 2021, Rotation of the convective core in γ Dor stars measured by dips in period spacings of g modes coupled with inertial modes. *Mon. Not. R. Astron. Soc.* **502**, 5856. DOI. ADS.

Santos, A.R.G., Godoy-Rivera, D., Finley, A.J., Mathur, S., Garcıa, R.A., Breton, S.N., Broomhall, A.-M.: 2024, *Kepler* main-sequence solar-like stars: surface rotation and magnetic-activity evolution. *Front. Astron. Space Sci.* **11**, 1356379. DOI. ADS

Sanz-Forcada, J., Micela, G., Ribas, I., Pollock, A.M.T., Eiroa, C., Velasco, A., Solano, E., García-Álvarez, D.: 2011, Estimation of the XUV radiation onto close planets and their evaporation. *Astron. Astrophys.* **532**, A6. DOI. ADS.

Schmitt, J.H.M.M., Schröder, K.-P., Rauw, G., Hempelmann, A., Mittag, M., González-Pérez, J.N., Czesla, S., Wolter, U., Jack, D., Eenens, P., Trinidad, M.A.: 2014, TIGRE: a new robotic spectroscopy telescope at Guanajuato, Mexico. *Astron. Nachr.* **335**, 787. DOI. ADS.

Schou, J., Antia, H.M., Basu, S., Bogart, R.S., Bush, R.I., Chitre, S.M., Christensen-Dalsgaard, J., Di Mauro, M.P., Dziembowski, W.A., Eff-Darwich, A., Gough, D.O., Haber, D.A., Hoeksema, J.T., Howe, R., Korzennik, S.G., Kosovichev, A.G., Larsen, R.M., Pijpers, F.P., Scherrer, P.H., Sekii, T., Tarbell, T.D., Title, A.M., Thompson, M.J., Toomre, J.: 1998, Helioseismic studies of differential rotation in the solar envelope by the solar oscillations investigation using the Michelson Doppler Imager. *Astrophys. J.* **505**, 390. DOI. ADS.

Scuflaire, R., Théado, S., Montalbán, J., Miglio, A., Bourge, P.-O., Godart, M., Thoul, A., Noels, A.: 2008, CLÉS, Code Liégeois d'Évolution Stellaire. *Astrophys. Space Sci.* **316**, 83. DOI. ADS.

See, V., Jardine, M., Vidotto, A.A., Petit, P., Marsden, S.C., Jeffers, S.V., do Nascimento, J.D.: 2014, The effects of stellar winds on the magnetospheres and potential habitability of exoplanets. *Astron. Astrophys.* **570**, A99. DOI. ADS.

Skumanich, A.: 1972, Time scales for Ca II emission decay, rotational braking, and lithium depletion. *Astrophys. J.* **171**, 565. DOI. ADS.

Soderblom, D.R.: 2010, The ages of stars. *Annu. Rev. Astron. Astrophys.* **48**, 581. DOI. ADS.

Tinetti, G., Drossart, P., Eccleston, P., Hartogh, P., Heske, A., Leconte, J., Micela, G., Ollivier, M., Pilbratt, G., Puig, L., Turrini, D., Vandenbussche, B., Wolkenberg, P., Pascale, E., Beaulieu, J.-P., Güdel, M., Min, M., Rataj, M., Ray, T., Ribas, I., Barstow, J., Bowles, N., Coustenis, A., Coudé du Foresto, V., Decin, L., Encrenaz, T., Forget, F., Friswell, M., Griffin, M., Lagage, P.O., Malaguti, P., Moneti, A., Morales, J.C., Pace, E., Rocchetto, M., Sarkar, S., Selsis, F., Taylor, W., Tennyson, J., Venot, O., Waldmann, I.P., Wright, G., Zingales, T., Zapatero-Osorio, M.R.: 2016, The science of ARIEL (Atmospheric Remote-sensing Infrared Exoplanet Large-survey) *SPIE* **9904**, 1X. DOI. ADS.

Varela, J., Brun, A.S., Strugarek, A., Réville, V., Zarka, P., Pantellini, F.: 2023, On Earth's habitability over the Sun's main-sequence history: joint influence of space weather and Earth's magnetic field evolution *Mon. Not. R. Astron. Soc.* **525**, 4008. DOI. ADS.

Vidotto, A.A., Gregory, S.G., Jardine, M., Donati, J.-F., Petit, P., Morin, J., Folsom, C.P., Bouvier, J., Cameron, A.C., Hussain, G.A.J., Marsden, S.C., Waite, I.A.: 2014, Stellar magnetism: empirical trends with age and rotation. *Mon. Not. R. Astron. Soc.* **441**, 2361. DOI. ADS.

Vidotto, A.A., Bourrier, V., Fares, R., Bellotti, S., Donati, J.F., Petit, P., Hussain, G.A.J., Morin, J.: 2023, The space weather around the exoplanet GJ 436b. II. Stellar wind-exoplanet interactions. *Astron. Astrophys.* **678**, A152. DOI. ADS.

Villaver, E., Livio, M.: 2009, The orbital evolution of gas giant planets around giant stars. *Astrophys. J. Lett.* **705**, L81. DOI. ADS.

Wilson, O.C.: 1968, Flux measurements at the centers of stellar H- and K-lines. *Astrophys. J.* **153**, 221. DOI. ADS.

Wilson, O.C.: 1978, Chromospheric variations in main-sequence stars. *Astrophys. J.* **226**, 379. DOI. ADS.

Wright, J.T.: 2018, Radial velocities as an exoplanet discovery method. In: Deeg, H.J., Belmonte, J.A. (eds.) *Handbook of Exoplanets* **4**. DOI. ADS.

Wright, N.J., Drake, J.J., Mamajek, E.E., Henry, G.W.: 2011, The stellar-activity-rotation relationship and the evolution of stellar dynamos. *Astrophys. J.* **743**, 48. DOI. ADS.

Zahn, J.P.: 1966, Les marées dans une étoile double serrée (suite). *Ann. Astrophys.* **29**, 489. ADS.

Zahn, J.-P.: 1977, Tidal friction in close binary stars. *Astron. Astrophys.* **500**, 383. ADS.

Publisher's Note Springer Nature remains neutral with regard to jurisdictional claims in published maps and institutional affiliations.